



## Structural and Optical Properties of Polymer Blend Nanocomposites Based on Poly (vinyl acetate-co-vinyl alcohol)/ TiO<sub>2</sub> Nanoparticles

A. Ismaila<sup>1</sup>, P. O. Akusu<sup>1</sup> and T. O. Ahmed<sup>2\*</sup>

<sup>1</sup>Department of Physics, Ahmadu Bello University, Zaria, Nigeria.

<sup>2</sup>Department of Physics, Federal University Lokoja, Kogi, Nigeria.

### Authors' contributions

*This work was carried out in collaboration between all authors. Authors TOA and POA designed the study. Author TOA wrote the protocol and wrote the first draft, while authors TOA and AI carried out the experimental work and analyses. Authors TOA and AI managed the literature searches. All authors read and approved the final manuscript.*

### Article Information

DOI: 10.9734/PSIJ/2015/4768

#### Editor(s):

(1) Daniel Beysens, OPUR International Organization for Dew Utilization, France.

(2) Abbas Mohammed, Blekinge Institute of Technology, Sweden.

#### Reviewers:

(1) Anonymous, Universiti Kebangsaan Malaysia, Malaysia.

(2) Anonymous, Ibn Tofail University, Morocco.

(3) Anonymous, Qinghai University for Nationalities, China.

Complete Peer review History: <http://sciencedomain.org/review-history/10067>

Original Research Article

Received 6<sup>th</sup> May 2013  
Accepted 10<sup>th</sup> March 2015  
Published 6<sup>th</sup> July 2015

### ABSTRACT

Titanium dioxide and organic polymer blend poly (vinyl acetate-co-vinyl alcohol) based nanocomposite membranes were prepared and their chemical structure, phase relationship and optical properties investigated. The Scanning Electron Microscopy (SEM) coupled with Energy Dispersive X-ray Spectroscopy (EDS) analysis reveals TiO<sub>2</sub> to be almost isomorphic (≥99% phase purity) with spherical particles having diameters in the range 25-40 nm. The composites were characterized by Fourier Transform Infrared (FTIR), SEM, X-Ray Diffraction (XRD) and Ultraviolet-visible (UV-vis) Spectrophotometry. The FTIR Spectroscopy reveals significant absorptions below 900 cm<sup>-1</sup> to represent Titanium bonds with organic groups and Oxygen while other prominent functional groups above 900 cm<sup>-1</sup> reflect the additivity of polyvinyl alcohol and polyvinyl acetate. It was found that embedding inorganic nanoparticles of TiO<sub>2</sub> into the polymer blend matrix of poly (vinyl acetate-co-vinyl alcohol) allowed for some crystallinity formation and cross-linking of the polymer composites during annealing. The XRD results show more defined peaks assigned to each phase of the composite as the TiO<sub>2</sub> content increases from 1 to 4% weight ratio, thus indicating that

\*Corresponding author: Email: [tajahmol@yahoo.co.uk](mailto:tajahmol@yahoo.co.uk), [tajahmol@gmail.com](mailto:tajahmol@gmail.com);

Nanoparticle filler remain in the semi-crystalline polymer matrix as a separate crystalline phase, which is in good agreement with the SEM. Finally, the resonant coupling between Ultraviolet-visible (UV-vis) light and the collective electronic transitions of polymer nanocomposites are examined using UV-vis Spectrophotometer. The variation in the percentage absorbance and transmittance over wavelength range 200 nm-900 nm is also attributed to TiO<sub>2</sub> Nanoparticles (Nps) content (1-4%) in the samples.

*Keywords: Polymer blend; TiO<sub>2</sub> nanoparticles; polymer nanocomposites; chemical structure; UV-visible light absorber.*

## 1. INTRODUCTION

In the last few years, the prospects for polymer blending have been compared to the alloying of metals because it requires little or no extra capital expenditure compared to the production of new polymers. This leverage has led to extensive use of polymer blends in the polymer industry over the last few years. Also, polymer blending offers the possibility of producing a range of polymeric materials with properties completely different from those of the blend constituents [1]. Blend properties are crucially affected by phase morphology and this in turn depends upon a number of factors including the choice of parent polymers, compatibilizers, blend composition, moisture content and the method of blend preparation [2,3]. Because of the significant interest in interfacial interaction between inorganic and organic phases (such as variety of polymer and their blend derivatives) as well as size-dependent phenomena of nanoscale particles, polymer blend nanocomposites are capable of dramatically improving numerous favorable properties without losing the inherent good properties of the polymer phases such as ductility, optical transparency etc. these advantages are never achieved in the conventional polymer composites. In addition, property enhancements in polymer nanocomposites are achieved at a very low loading (<5 wt %) of inorganic nanoparticles while the conventional polymer composites (polymer containing microparticles/micron-sized particles as fillers) usually require much loading of the order of 25-40 wt % [4].

In contrast to the traditional dyes, inorganic semiconductive nanocrystals have more resistant to chemical attacks and low degradation with higher photobleaching, broader excitation wavelength range, narrower and tunable emission spectra [5,6,7,8]. This influence has attracted an enormous research effort leading to a myriad of potential applications in engineering, medicine, biology, electronics and allied

industries. Their optical properties have been the center of attraction due to strong size-dependent quantum confinement effect associated with inorganic semiconductive nanocrystals. For the development of novel nanodevices such as electronics and optical devices, various stabilizers (surfactants, polymers or coupling agents) have been employed to modify the surface functionalities of the nanocrystals [9,10], as these nanocrystals are seldom prepared without aggregation. A great deal of attention has been focused on TiO<sub>2</sub> in contrast to other semiconducting materials, because of its low cost, non-toxicity, chemical stability, resistance to photocorrosion, high photocatalytic activity and high refractive index [11,12]. In the last decade, most studies are mainly focused on the dispersion of nanocrystalline TiO<sub>2</sub> powder for photocatalysis compared to TiO<sub>2</sub> thin films due to its higher photocatalytic activity [13]. It is an established fact that a mixture of anatase TiO<sub>2</sub> and a small percentage of rutile TiO<sub>2</sub> give optimal photocatalytic efficiency as the anatase phase has a wider band gap of 3.20 eV [14].

Polymer nanocomposites represent a merger between traditional organic and nanosized inorganic materials, resulting in compositions that are truly hybrid. The key to forming such novel materials is adequate understanding and manipulation of the guest-host chemistry, occurring between the polymer and the nanoparticles, in order to obtain a homogenous dispersion and a good contact between polymer and added particle surfaces [15]. Generally, the resultant nanocomposites display enhanced favorable properties such as conductivity, toughness, optical activity, catalytic activity, chemical selectivity etc [16]. These attributes have led to the growing interest and uses in various fields such as military equipments, safety and protective garments, automotive, aerospace, electronic and optical devices. A lot of research works exploiting these aforementioned properties have been carried out for possible applications including flame retardancy, chemical resistance,

UV resistance, electrical conductivity, environmental stability, water repellency, magnetic field resistance, radar absorption etc [17,18,19,20,21].

In this paper, we report the development of Poly (vinyl acetate-co-vinyl alcohol)/ TiO<sub>2</sub> nanocomposites achieved via a two-stage synthetic route and the relationship between structural and optical properties of the resulting hybrid Poly(vinyl acetate-co-vinyl alcohol)/ TiO<sub>2</sub> nanocomposites employing Fourier Transform Infrared (FTIR) spectroscopy, Scanning Electron Microscopy (SEM), X-Ray Diffraction (XRD) analysis and UV-visible Spectrophotometry.

## 2. MATERIALS AND METHODS

Poly (vinyl acetate-co-vinyl alcohol)/ TiO<sub>2</sub> nanocomposites were produced via a two-stage reaction involving the synthesis of TiO<sub>2</sub> Nanoparticles (Nps) from titanium (IV) chloride {TiCl<sub>4</sub>, BDH Limited Poole, England} employing hydrothermal technique and subsequent mixing of modified TiO<sub>2</sub> Nps with Poly(vinyl acetate-co-vinyl alcohol) dissolved in toluene via one-pot reaction. Surface morphology of the synthesized TiO<sub>2</sub> nanoparticles was observed using EVOI MA10 (ZEISS) multipurpose scanning electron microscope operating at 20kV employing secondary electron signals. Four samples of Poly (vinyl acetate-co-vinyl alcohol)/ TiO<sub>2</sub> nanocomposites containing 1-4% of TiO<sub>2</sub> Nps were produced by solution casting into Petri dishes. The samples were oven dried at temperature lower than the melting point of the polymer blend for 12 hrs and subsequently flat and uniform thin samples were obtained. The FTIR spectra of all the component reagents, polymer blend and the prepared nanocomposite samples were obtained using SHIMADZU FTIR-8400S Spectrophotometer in transmission mode without KBr. The spectra were recorded in the frequency range from 400 to 4600 cm<sup>-1</sup>, after 25 scans, with resolution of 2 cm<sup>-1</sup>. The positions and intensities of the IR bands were processed with Spectral Analysis software.

Surface morphologies of Poly (vinyl acetate-co-vinyl alcohol)/ TiO<sub>2</sub> nanocomposites were observed using EVOI MA10 (ZEISS) multipurpose scanning electron microscope operating at 20kV employing secondary electron signals at a magnification of 500X and the particle size distribution was obtained using imaging software (Image-J). The crystallinity of polymer blend/ TiO<sub>2</sub> nanocomposites was

observed using X-Ray Diffractometer (Phillips X'pert Pro X-Ray Diffractometer) employing a 1.54060Å copper X-ray source. The samples were scanned from 2θ = 5°-80° using a step size of 0.06°. The percentage crystallinity (X<sub>c</sub>) was calculated following the procedure proposed by [22], with the Scientific Graphing and Data Analysis Software (Origin 8.0), using the following equation:

$$X_c = \frac{A_c}{A_c + A_a}$$

where X<sub>c</sub>, (percentage crystallinity), is the ratio of crystalline peak area (A<sub>c</sub>) to the sum of the crystalline peak area (A<sub>c</sub>) and amorphous peak area (A<sub>a</sub>). Finally, the absorption/filtering property of the polymer blend /TiO<sub>2</sub> nanocomposites was studied in the ultraviolet (UV) radiation wavelength range of 200 nm - 400 nm and visible radiation wavelength range of 400 nm - 900 nm using JENWAY 6405 UV-visible Spectrophotometer.

## 3. RESULTS AND DISCUSSION

The image presented in Fig. 1 together with the corresponding EDS spectra obtained using characteristic x-rays emitted by TiO<sub>2</sub> nanoparticles was observed at a magnification of 83.04kX. The uniform contrast in the image revealed TiO<sub>2</sub> to be almost isomorphous. Nevertheless, Oxygen and Nitrogen occur with minor concentrations as impurities thereby making Ti the dominant element with concentration of about 99.5% as depicted in the EDS spectra (Fig. 1b). The morphology of TiO<sub>2</sub> nanoparticles is such that the particles are closely packed and spherical in shape. The average diameter of the particles is in the range of 25-40 nm reflecting that TiO<sub>2</sub> nanoparticles are transparent and suitable filler for polymer composite applications.

The spectra for the functionalized TiO<sub>2</sub> nanoparticles, poly (vinyl alcohol), poly (vinyl acetate), polymer blend [poly (vinyl acetate-co-vinyl alcohol)] and the functionalized TiO<sub>2</sub> are given in Figs. 2(a-d). It is an established fact that the fundamental vibrations of solids (finger prints) are localized in the low frequency region (<1200 cm<sup>-1</sup>) of the midrange (400-4000 cm<sup>-1</sup>) of the infrared (IR) spectrum. Also, as reported by [23], the Ti-O bond is clearly located in the range from 400-900 cm<sup>-1</sup>. In this work, the significant absorptions observed below 900 cm<sup>-1</sup> represent

Ti bonds with vinyl groups, secondary alcohols, carbonyl groups and oxygen. The prominent functional groups in poly (vinyl alcohol), poly (vinyl acetate) and their blend are OH stretching vibrations,  $\text{CH}_2$  stretching and bending vibrations,  $\text{CH}_3$  bending vibrations, C-O-C vibration in esters,  $\nu\text{C}=\text{O}$  stretching vibration, C-OH stretching vibrations, CH bending and C=O stretching vibration.

From Figs. 3(a-d), it can equally be deduced that the OH stretching vibrations of the intermolecular hydrogen bonding occurring in the range  $3427.62\text{ cm}^{-1}$ - $3483.56\text{ cm}^{-1}$  is basically due to the adsorbed H-O-H. Organics (methylene groups) are also represented by the  $\nu_{\text{as}}\text{-CH}_2$  asymmetrical stretching vibrations in ranges slightly above  $2910\text{ cm}^{-1}$ . The CH stretching vibrations with coexisting terminal triple bonds resulting from remnant alkynes occur in the range  $2067.76\text{ cm}^{-1}$  -  $2145.88\text{ cm}^{-1}$ . All the changes observed in the vibration frequency of  $\nu\text{C}=\text{O}$  in the blend indicates that the incorporation of the nanofillers ( $\text{TiO}_2$ ) has great

influence on the vibration frequency of  $\nu\text{C}=\text{O}$ . Furthermore, conjugation with  $\text{CH}_3$  (phenyl groups) results in an increase in bond length of C=O thereby creating functional sites on the surface of the polymer blend. The C-O-C vibrations in esters occurring in the frequency ranges  $949.01\text{ cm}^{-1}$  -  $950.94\text{ cm}^{-1}$  and  $1284.63\text{ cm}^{-1}$  -  $1293.31\text{ cm}^{-1}$  represent the possible combination of acetate and alcohol groups. Finally, the functional groups appearing in the range  $383.85\text{ cm}^{-1}$  -  $491.66\text{ cm}^{-1}$  represent Ti-O bonds of the functionalized  $\text{TiO}_2$  nanoparticles. The observed spectra of the polymer-blend/ $\text{TiO}_2$  nanocomposites reveal the additivity of the spectra of polyvinyl alcohol and poly vinyl acetate with the modified  $\text{TiO}_2$  Nps. In Figs. 3(a) and 3(b), most of the functional groups peculiar to the component reagents were observed but in Figs. 3(c) and 3(d), chemical reactions between the component reagents and the increase in the concentration of the functionalized  $\text{TiO}_2$  nanoparticles from 2%-4% are responsible for the extinction of the functional groups as a result of oxidation and hydrolysis.

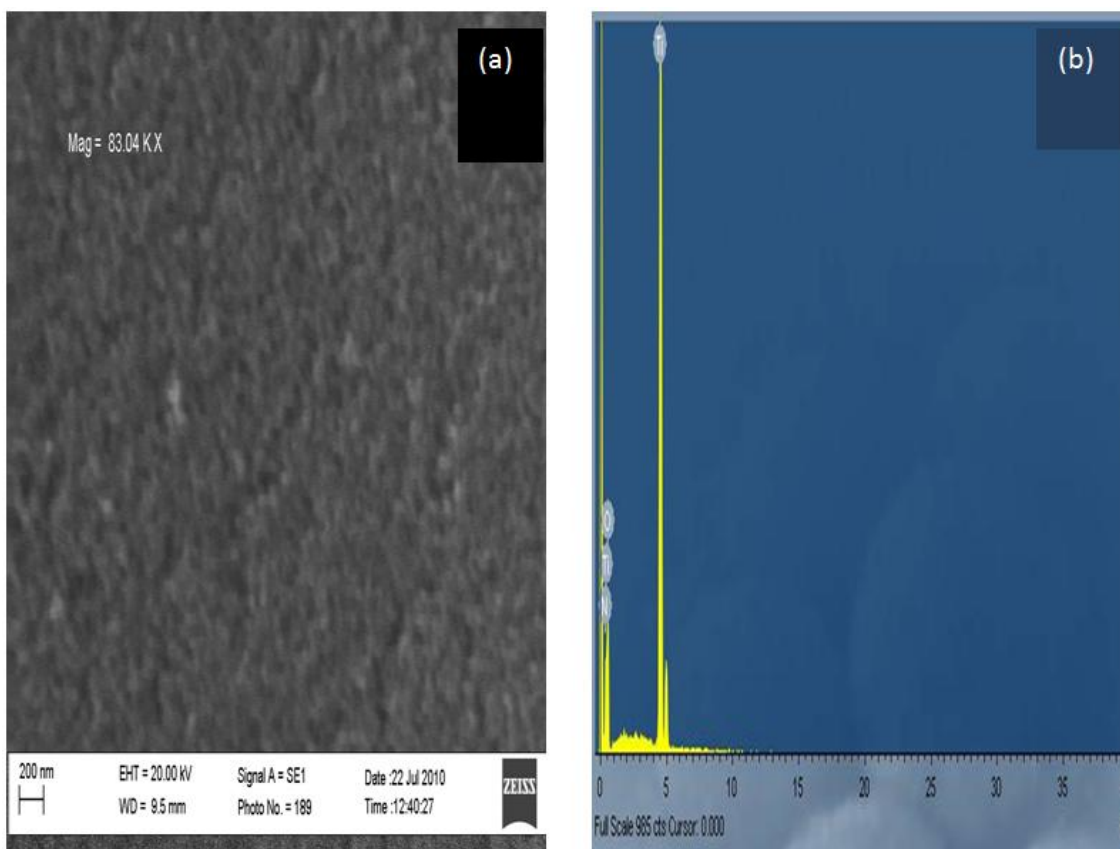


**Fig. 1. Microstructure and elemental composition of  $\text{TiO}_2$  Nps: (a) SEM image of  $\text{TiO}_2$  Nps (b) EDS spectra of  $\text{TiO}_2$  Nps**

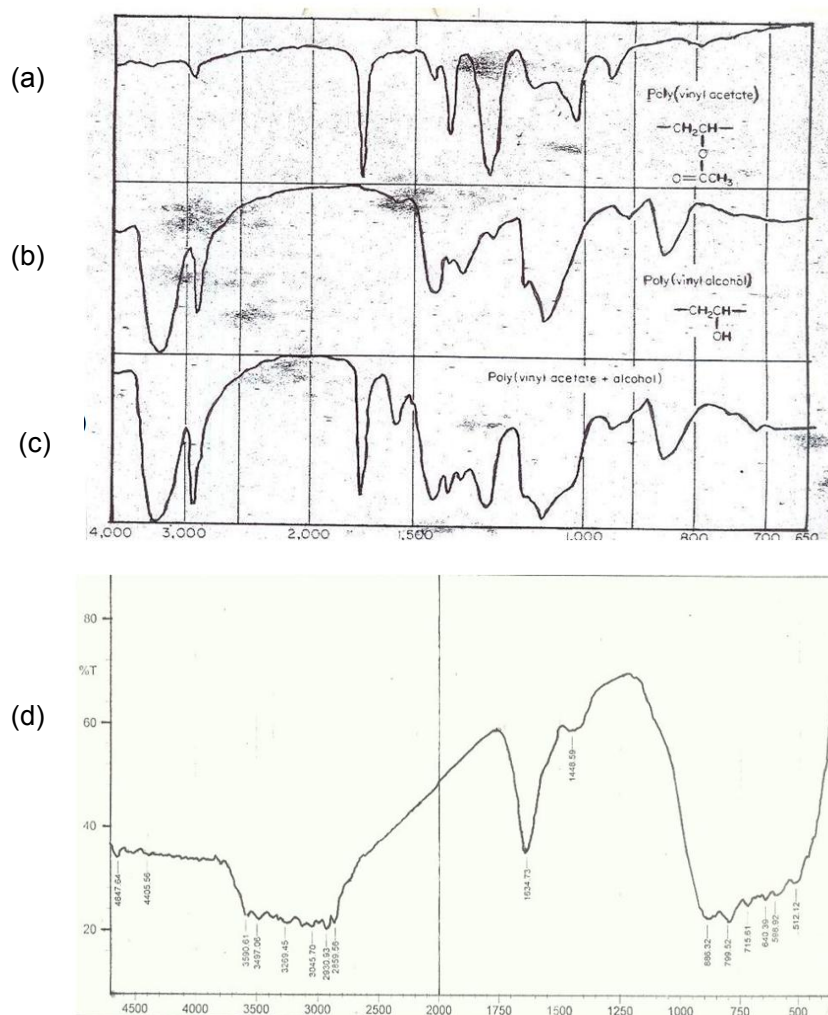


**Fig. 2. FTIR Spectra of (a) Poly (vinyl alcohol), (b) Poly (vinyl acetate), (c) Polymer blend [poly (vinyl acetate-co-vinyl alcohol)] and (d) functionalized TiO<sub>2</sub> Nps**

The uneven baseline in the XRD patterns seen in Figs. 4 (a-d) for all the samples is due to the large amount of amorphous polymer content. The addition of TiO<sub>2</sub> nanoparticles to the polymer blends improved the crystallinity of the composites. The diffraction peaks in the range  $2\theta = 15^\circ$ - $20^\circ$  can be linked to crystalline behaviour of the polymer blends. The peaks at  $2\theta = 19.66^\circ$ ,  $19.84^\circ$ ,  $20.34^\circ$ , and  $20.49^\circ$  with d-spacings  $d = 4.5154\text{\AA}$ ,  $4.4742\text{\AA}$ ,  $4.3642\text{\AA}$  and  $4.3325\text{\AA}$  indicate the presence of crystalline structure of PVA, consistent with the works of [24,25]. Furthermore, the XRD patterns of polymer blend/ TiO<sub>2</sub> nanocomposites reveal the presence of TiO<sub>2</sub> phase but few peaks representing TiO<sub>2</sub> phase have been shifted slightly to lower  $2\theta$  values ( $2\theta = 21.91^\circ$ ,  $22.13^\circ$ ,

$22.37^\circ$ ,  $22.45^\circ$ ,  $22.78^\circ$ ,  $22.80^\circ$  and  $22.99^\circ$ ) due to slight expansion of TiO<sub>2</sub> crystal structure as a result of surface modification and bonding with the polymer blend matrix. This is also consistent with the results presented in some literatures [26,27]. The average crystallite size corresponding to structural order of the pattern determined from integral breadth of the peaks according to Scherrer's equation [28] have values ranging from  $1688\pm 290$  nm to  $4589\pm 130$  nm. The percentage crystallinity values of the polymer blend/ TiO<sub>2</sub> nanocomposites following the procedure proposed by [22] range from  $56.9\pm 0.2\%$  to  $67.6\pm 0.7\%$ . The sample with 4% TiO<sub>2</sub> content displayed higher percentage crystallinity compared to other samples.

The microstructure of the polymer blend/TiO<sub>2</sub> nanocomposites reveals two distinct phases comprising of lighter modified TiO<sub>2</sub> nanoparticles and dark bulk polymer blend matrix. The lighter modified TiO<sub>2</sub> nanoparticles are evenly dispersed over the dark bulk polymer matrix with spherical shapes and the concentration increased with increasing content of the modified TiO<sub>2</sub> NPs (1%-4%) as depicted in Figs. 5(a-d). The contrast observed in the SEM images [Figs. 5(a-d)] arises from atomic number difference, since phases within a material are dependent upon back

scattered electron yield and the corresponding atomic number of atoms present within different phases. As such, the modified TiO<sub>2</sub> nanoparticles appear lighter compared to the bulk polymer blend matrix because the atoms present in TiO<sub>2</sub> phase have higher atomic numbers and higher back scattered electron yield. The average particle diameters of the polymer-blend/TiO<sub>2</sub> nanocomposites as determined from SEM images using imaging software (Image J) range from 119±5 μm to 179±4 μm.

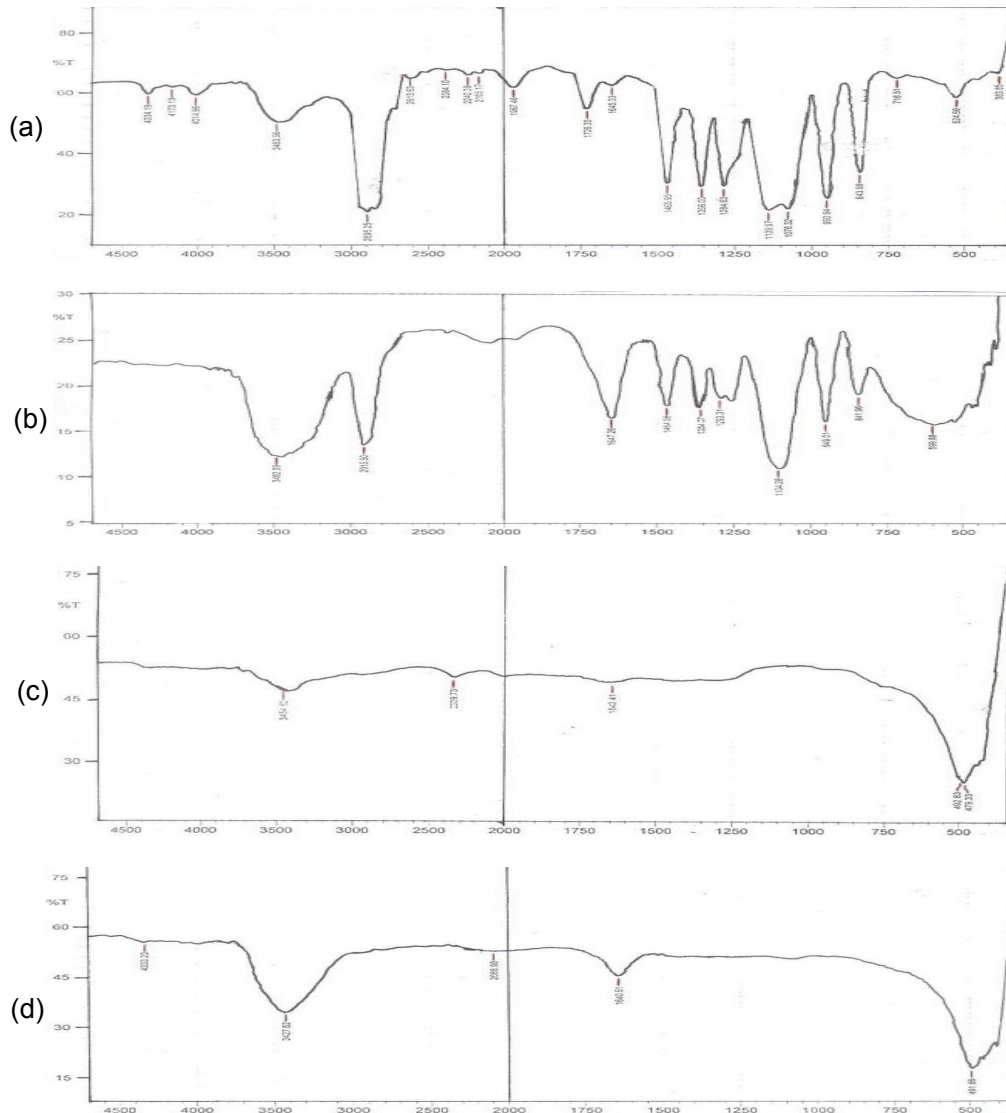


**Fig. 3. FTIR Spectra of Polymer blend/ TiO<sub>2</sub> Nanocomposites containing: (a) 1% of TiO<sub>2</sub> Nps (b) 2% of TiO<sub>2</sub> Nps (c) 3% of TiO<sub>2</sub> Nps and (d) 4% of TiO<sub>2</sub> Nps**

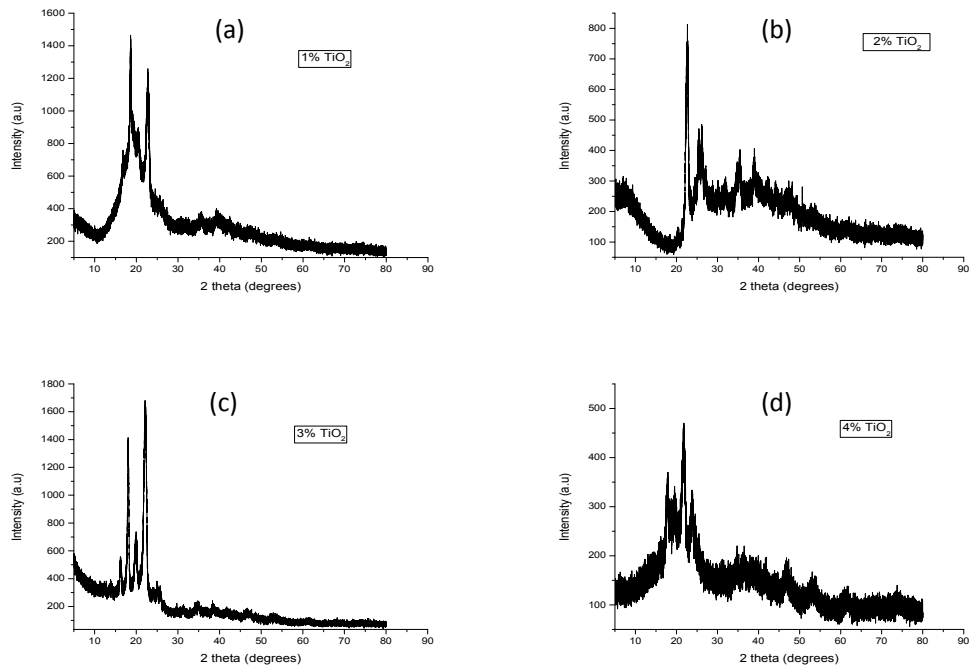


**Fig. 4. X-ray diffraction patterns of polymer blend/TiO<sub>2</sub> nanocomposites containing (a) 1% of TiO<sub>2</sub>, (b) 2% of TiO<sub>2</sub>, (c) 3% of TiO<sub>2</sub> and (d) 4% of TiO<sub>2</sub>**

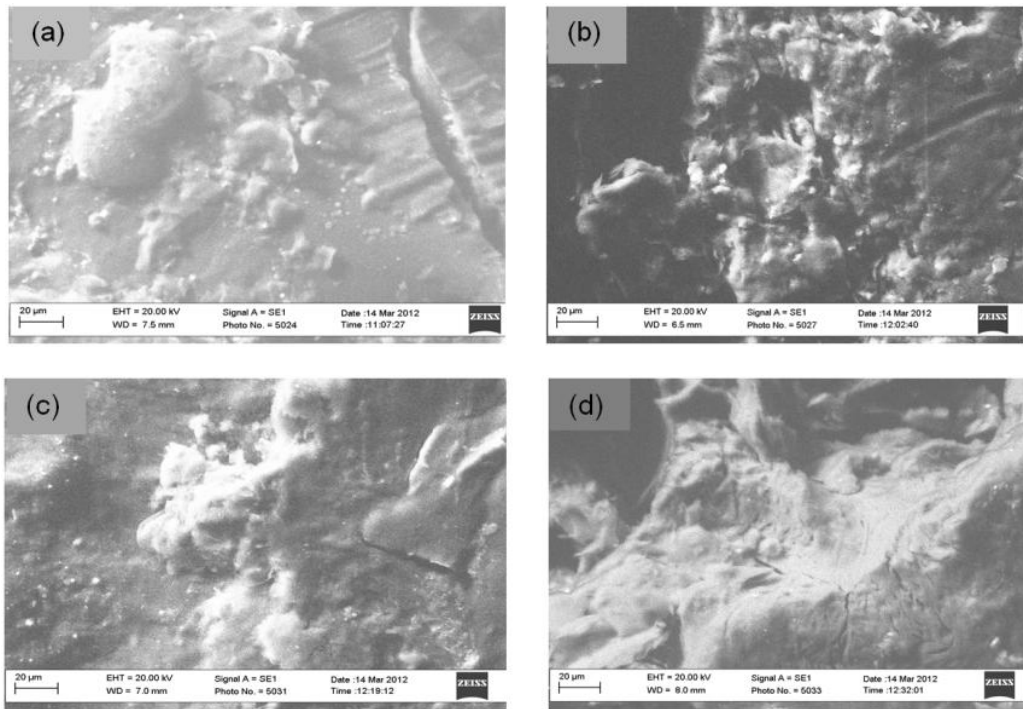


**Fig. 5. SEM Images of polymer blend/TiO<sub>2</sub> nanocomposites containing: (a) 1% of TiO<sub>2</sub>, (b) 2% of TiO<sub>2</sub>, (c) 3% of TiO<sub>2</sub> and (d) 4% of TiO<sub>2</sub>**

It is a well known fact that changes occur when atoms or impurities are incorporated into a pure matrix (polymer, semiconductor, metal etc), because their environment is neither inert nor isotropic. Subsequently, exposing the anisotropic matrix (polymer nanocomposites) to UV-vis light may lead to resonant coupling between the photons (in this case, UV-vis component of the electromagnetic spectrum) and the collective modes (electronic transitions/excitations) of the polymer nanocomposites. The interaction of the UV-visible light with the polymer nanocomposites possibly will give rise to polarization of the nanocomposite matrix, which in turn can be seen as variation in the magnitude of absorption/transmission with respect to changes in wavelengths (i.e. 200-900 nm) when examined using UV-vis spectrophotometer. In addition to this, anisotropy of the nanocomposite matrix resulting from addition of TiO<sub>2</sub> nanoparticles gave rise to varied properties as a result of slight structural modifications. The slight variation in the percentage absorbance over wavelength range (i.e. 200-900 nm) is attributed to the TiO<sub>2</sub> nanoparticles content (1-4%) in each sample.

The UV-VIS spectra of polymer blend/TiO<sub>2</sub> nanocomposites are given in Figs. 6(a-d). The

plot for polymer blend/TiO<sub>2</sub> sample (containing 1 wt % of nanoparticles) is presented in Fig. 6(a). The sample filters at the onset of ultraviolet radiation wavelength through 295 nm above which it absorbs significantly and rapidly until maximum absorbance of 1.4% is recorded at a wavelength of 390 nm. Slightly above the visible range, there is little decline in absorbance but appreciates reasonably through the whole range with maximum recorded at a wavelength of approximately 500nm. The sample displayed excellent property of being an ultraviolet radiation filter at low wavelengths (<300 nm) and absorber at higher wavelengths (300-400 nm) of the UV range in addition to being an excellent visible absorber. Fig. 6(b) portrays the behaviour for polymer blend sample containing 2 wt % of TiO<sub>2</sub> nanofillers. The spectrum shows absolute transparency from the onset of ultraviolet radiation wavelength range through a visible wavelength of 515 nm. A much significant absorbance of approximately 3.0%, the maximum, is recorded slightly above that (i.e. at 520 nm) from which the absorbance decreases very slightly with a minimum of 2.7% at 800 nm. This material is an excellent UV filter and a very good visible radiation absorber.

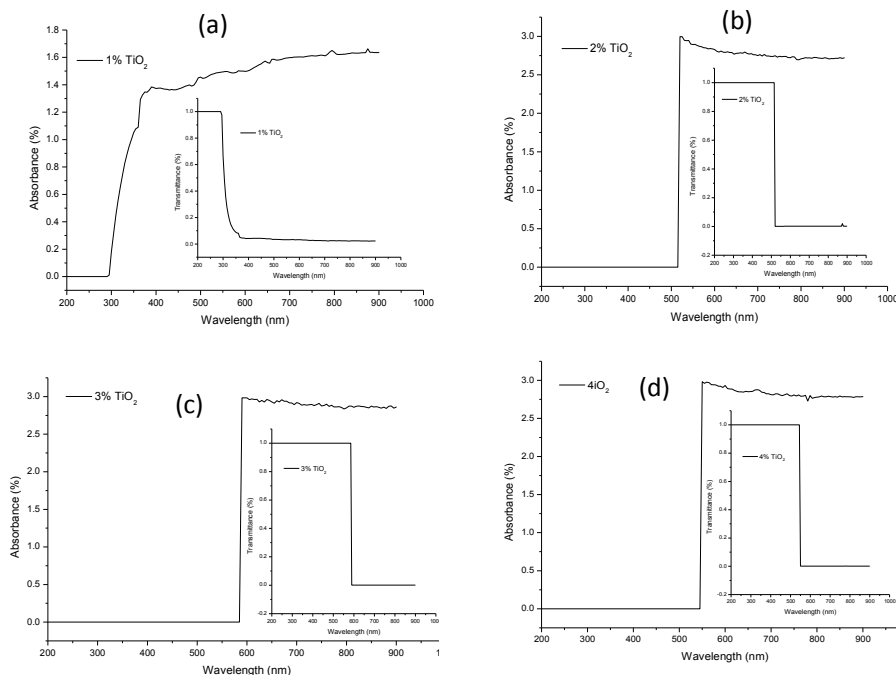


**Fig. 6. UV-vis spectra of polymer-blend/TiO<sub>2</sub> nanocomposites containing: (a) 1% of TiO<sub>2</sub>, (b) 2% of TiO<sub>2</sub>, (c) 3% of TiO<sub>2</sub> and (d) 4% of TiO<sub>2</sub>**



A similar behaviour to the polymer blend samples described above is observed in both the remaining blend samples (with 3 wt % and 4 wt % of TiO<sub>2</sub> nanofillers respectively) as depicted in Figs. 6(c) and 6(d). However, there are slight shifts in the onsets of absorption, with the sample containing 3 wt % of TiO<sub>2</sub> having onset at a wavelength of 590 nm corresponding to maximum absorbance of approximately 3.0% and that containing 4 wt % of TiO<sub>2</sub> having onset at 550 nm corresponding to maximum absorbance of 2.9% as well. The minimum absorbance for these samples are recorded at 795 nm (2.8%) and at 780 nm (2.7%) respectively. These shifts are attributed to higher content of TiO<sub>2</sub> nanofillers in the polymer blends as TiO<sub>2</sub> are transparent to UV-vis light.

#### 4. CONCLUSION

The development of the polymer blend nanocomposites was realized by surface modification of TiO<sub>2</sub> Nps in order to create functional sites and improve dispersion of nanoparticles in the polymer blend matrices. FTIR spectroscopy proved the existence of covalent chemical bonding between the polymer chains and inorganic phase in the polymer blend nanocomposites. Thus, revealing significant absorptions below 900 cm<sup>-1</sup> to represent titanium bonds with organic groups and oxygen while other prominent functional groups above 900cm<sup>-1</sup> reflect the additivity of polyvinyl acetate and polyvinyl alcohol. X-ray diffraction analysis of the polymer blend nanocomposites revealed an increase in the percentage crystallinity from 56.9±0.2% to 67.6±0.7% for the polymer-blend nanocomposites as TiO<sub>2</sub> nanoparticles content increases from 1% to 4%. Observations from SEM analysis showed that the dispersion of TiO<sub>2</sub> nanoparticles in the polymer matrix was relatively uniform with particles having good adhesion with polymer domains. Investigation with UV-visible spectrophotometer revealed that the dispersion of TiO<sub>2</sub> nanoparticles improved the optical properties of the polymer blends. The fact that nanocomposites displayed some level of transparency at lower wavelengths indicates that the nanoparticles are not agglomerated. In addition, strong UV absorption in some of the nanocomposite samples was observed because of the incorporated TiO<sub>2</sub> particles. In fact, with the exception of sample with 1% content of nanoparticles, all the samples transmit UV radiation and absorb visible radiation at wavelengths of 520 nm, 590 nm and 550 nm respectively. Thus the developed polymer blend

nanocomposites could act as an efficient optically transparent UV filter and visible radiation absorber.

#### ACKNOWLEDGEMENTS

We thank Physics Advanced Laboratory, Sheda Science and Technology Complex, Abuja, Nigeria, National Research Institute for Chemical Technology, Zaria, Nigeria and the Multi-users Laboratory, Department of Chemistry, Ahmadu Bello University, Zaria, Nigeria for technical assistance during the experimental characterization.

#### COMPETING INTERESTS

Authors have declared that no competing interests exist.

#### REFERENCES

1. Wanchoo RK, Sharma PK. Viscometric study on the compatibility of some water soluble polymer-polymer mixtures. *Euro. Polym. J.* 2003;39:1481-82.
2. Dyson RW. *Engineering polymers*. Chapman and Hall, New York. 1990;20-28.
3. Chuu MS, Meyers RR. Effect of moisture content on the dielectric behaviour of Poly (vinyl acetate)-natural rubber blend. *J Appl Polym Sci.* 1987;34(4):1447.
4. Saujanya C, Radhakrishna S. Polymer nanocomposites. *J. of Polym. Sci.* 2001; 42:6723-6731.
5. Riegler J, Ditengou F, Palme K, Nann T. Blue shift of CdSe/ ZnS nanocrystals-labels upon DNA-hybridization. *J. Nanobiotechnol.* 2008;6(1):7.
6. Bruchez Jr. M, Moronne M, Gin P, Weiss S, Alivisatos AP. Semiconductor nanocrystals as fluorescent biological labels. *Science.* 1998;281(5385):2013-2016.
7. Chan WCW, Nie S. Quantum dot bioconjugates for Ultrasensitive Nonisotopic Detection *Science.* 1998; 281(5385):2016–2018.
8. Jaiswal J, Mattoussi H, Mauro J, Simon S. Long-term multiple color imaging of live cells using quantum dot bioconjugates. *Nat. Biotechnol.* 2003;21(1):47–51.
9. Patra MK, Manoth M, Singh VK, Gowd GS, Choudhry VS, Vadera SR, Kumar N. Synthesis of stable dispersion of ZnO quantum dots in aqueous medium showing

- visible emission from bluish-green to yellow. *J. Lumin.* 2009;129(3):320–324.
10. Guo Z, Kumar C, Henry LL, Domes EE, Hormes J, Podlaha EJ. Displacement synthesis of Cu shells surrounding Cu nanoparticles. *J. Electrochem. Soc.* 2005; 152(1):D1–D5.
  11. Legrini O, Oliveros E, Braun AM. Photochemical processes for water treatment. *Chem. Rev.* 1993;93(2): 671-698.
  12. Sugimoto T, Zhou X, Muramatsu A. Synthesis of uniform anatase TiO<sub>2</sub> nanoparticles by gel-sol method: 3. formation process & size control. *J. Colloid Interface Sci.* 2003;259(1):43-52.
  13. Jianguo Y, Jimmy CYU, Cheng B, Zhao X. Photocatalytic activity & characterization of the sol-gel derived Pb-doped TiO<sub>2</sub> thin-films. *J. Sol-Gel Sci. Tech.* 2002;24(1): 39-48.
  14. Bouras P, Stathatos E, Lianos P. Pure versus metal-ion-doped nanocrystalline titania for photocatalysis. *Appl. Catal. B: Environ.* 2007;73(1-2):51-59.
  15. Lagashetty A, Venkataramen I. *Polymer nanocomposites.* John Wiley and Sons; 2005.
  16. Garcia C, Maria M, Dela L. *Polymer-inorganic nanocomposites: Influence of colloidal silica,* A PhD thesis submitted to the University of Twente. Netherlands; 2004.
  17. Mohan S, Lauren NC, Surya SG, Karen IW. Melt intercalation of polystyrene in layered silicates. *J. of Polym. Sci.: Part B: Polym. Physics.* 1996;34:1433-1449.
  18. Lee SS, Lee CS, Kim MH, Kwak SY, Park M, Lim S, Choe CR, Kim J. Specific interaction governing the melt intercalation of clay with Poly(styrene-co-acrylonitrile) copolymers. *J. of Polym. Sci.: Part B: Polym. Physics.* 2001;39:2430-2435.
  19. Pegoretti A, Dorigato A, Penati A. A tensile mechanical response of polyethylene-clay nanocomposites. *Express Polymer Letters.* 2007;1(3):123-131.
  20. Tolstov AL, Matyushov VF, Klymchok, DO. Synthesis and characterization of hybrid cured poly (ether-urethane) Acrylate/Titania microcomposites formed from tetraalkoxy titanate precursors. *Express Polymer Letters.* 2008;2(6):449-459.
  21. Manias E, Zhang J, Huh JY. Polyethylene nanocomposite heat sealants with a versatile peelable character. *Macromol. Rapid Commun.* 2009;30:17-23.
  22. Eichhorn SJ, Young RJ. The young's modulus of microcrystalline cellulose. *Cellulose.* 2001;8:197-207.
  23. Morterra C, Magnacca G. A case study: Surface chemistry & structure of catalytic aluminas as studied by vibrational spectroscopy of adsorbed species. *Catal. Today.* 1996;27:(3-4):497-532.
  24. G'eminarda JC, Bonraya DH. Thermal conductivity associated with a bead-bead content decorated by a liquid bridge; an experimental study based on the response of a chain subjected to thermal cycles. *Gayvallet Eur, Phys.* 2005;48: 509-17.
  25. Lee GW, Park M, Kim J, Lee JI, Yoon HG. Enhanced thermal conductivity of polymer Composites filled with hybrid filler. *Composites Part A: Applied Science and Manufacturing.* 2006;37:727-734.
  26. Shuqiang J, Hongmin Z. Electrolysis of Ti<sub>2</sub>CO Solid Solution Prepared by TiC & TiO<sub>2</sub>. *Journal of Alloys & Compounds.* 2007;438:243-246.
  27. Yang Z, Choi D, Kerisit S, Rosso KM, Wang D, Zhang Z, Graffi G, Liu J. Nanostructures and lithium electrochemical reactivity of lithium titanates and titanium oxides: A review. *Journal of Power Sources.* 2009;192(2):588-598.
  28. Patterson AL. The Scherrer formula for X-ray particle size determination. *Physical Review.* 1939;56(10):978-982.

© 2015 Ismaila et al.; This is an Open Access article distributed under the terms of the Creative Commons Attribution License (<http://creativecommons.org/licenses/by/4.0>), which permits unrestricted use, distribution, and reproduction in any medium, provided the original work is properly cited.

*Peer-review history:*  
*The peer review history for this paper can be accessed here:*  
<http://sciencedomain.org/review-history/10067>